International Journal of Analytical, Experimental and Finite Element Analysis (IJAEFEA), Issue. 2, Vol. 2, June 2015.
e-ISSN: 2394-5141, p-ISSN: 2394-5133, pp 89-94

Modeling Cylindrical Dipole Antenna by Finite Element Method at 2400MHz

E. El Kennassi
essaid.elkennassi@orange.fr

K. Janati Idrissi
khalid.janati.id02@gmail.com

L. Bousshine
lbousshine@yahoo.fr

Laboratoire des Technologies de Construction et Systèmes Industriels (LTCSI), Mechanics Department, ENSEM, Hassan II University of Casablanca, Ain Chock, Casablanca, Morocco.

***Abstract*—Finite element method is used for the electric field computation of a dipole antenna at the 2400 MHz frequency in the context of Dirichlet and absorbing boundary conditions. It shows that the electric field pattern, both in bi-dimensional and polar plots, has an omnidirectional property for the dipole antenna. Our results are compared against the method of moments with a good agreement.**

***Index Terms*—**finite element method, antennas, electromagnetic field, Galerkin, excitation, scattering problem, method of moments.

I. Introduction

The finite element method (FEM) is very important for engineers, because the fact that solving problems is simulated to approach the reality. We can predict behavior of physical phenomena by using actual computers capacities. Indeed, for engineer sciences, we create a mathematical model following four steps: (i) building a geometry, (ii) discretizing the obtained domain, (iii) solving the governing equations, and (iv) dealing with the appropriate results [1, 2].

The engineers have to obtain a solution in which time resources and creativity are the ultimate aims. To investigate the electromagnetic field created near high frequency structures, we have to establish several parameters and given that the geometry is complex the solution of equations governing the system is achieved through the use of numerical tools.

We proceed to model the electromagnetic field radiated by a 2400MHz dipole antenna using FEM where we minimize the weighted residual, i.e., to have a lowest error [1,3-6]. We use a Perfect Electric Conductor model (PEC) for the antenna [1], and we generate the electromagnetic field with a source of excitation current J_z along z-direction over the dipole feed. Then, using Maxwell's equations [1, 7] we obtain the wave equation which models the electric field. Thus, the incident wave to the cylindrical antenna is a transverse magnetic plane wave along the z-axe. This wave interacts with the excited structure and can be modeled as a scattering problem.

The plan of this work is as follow: first (section II), we describe the mathematical model proposed to deal with a cylindrical dipole antenna by FEM at 2400MHz frequency, second (section III), we present and discuss our results, and compare them with other results, particularly the Method of Moment (MoM), and we end with conclusion.

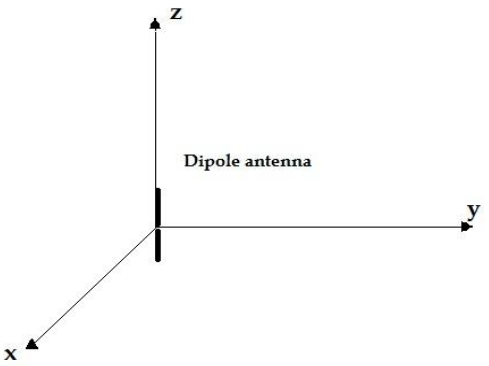

Figure 1. Dipole antenna

II. Method and Numerical Experience

A. Inhomogeneous Scalar Wave Equation

A uniform transverse magnetic plane wave TM_z is incident wave over the cylindrical antenna which has the radius a. The electric field is given by,

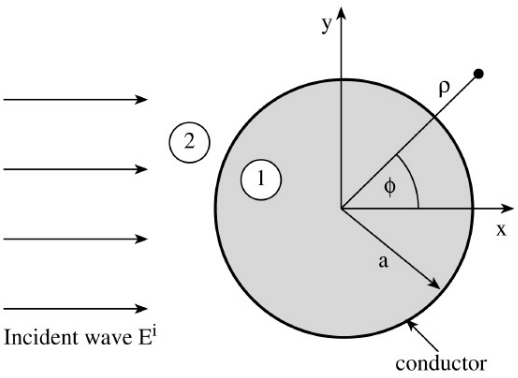

Figure 2. Incident plane wave over the PEC cylindrical antenna [7]

$$\overrightarrow{E^i} = \hat{a}_z E_0 e^{-jk_0 x} = \hat{a}_z E_0 e^{-jk_0 \rho \cos\phi}. \quad (1)$$

where the incident plane wave over the antenna is oriented according to x-axe. Note that $\hat{a}_z$ is the unit vector along the z-direction, E_0 is the plane wave amplitude, k_0 is the propagation constant in free space, ρ is the radial distance between the center cylinder and the observation point, and ϕ the corresponding angle measured from the positive x-axe, as shown in Fig. 1 and Fig. 2.

The total field (incident and scattered field) is obtained at a distance ρ=60 mm to the cylinder center. This problem is governed by the time-harmonic Maxwell's equations [1, 7]. The total electric field is z-directed, then, there will be no field variations along the z-direction,

$$\frac{\partial E_z}{\partial z} = 0. \quad (2)$$

The wave equation governing this structure is given by the well-known inhomogeneous Helmholtz equation or inhomogeneous scalar wave equation with non-zero right hand side term [1]

$$\frac{\partial}{\partial x}\left(\frac{1}{\mu_r}\frac{\partial E_z}{\partial x}\right) + \frac{\partial}{\partial y}\left(\frac{1}{\mu_r}\frac{\partial E_z}{\partial y}\right) + k_0^2 \varepsilon_r E_z = j\omega\mu_0 J_z \quad (3)$$

Thus, the Galerkin's Technic [5] for solving this type of second order partial differential (3) is shown below.

B. Galerkin's Technic

In order to have a Galerkin like-equation,

$$\frac{\partial}{\partial x}\left(\alpha_x \frac{\partial u}{\partial x}\right) + \frac{\partial}{\partial y}\left(\alpha_y \frac{\partial u}{\partial y}\right) + \beta u = g, \quad (4)$$

we assume from (3) that

$$u = E_z,\ \alpha_x = \alpha_y = \frac{1}{\mu_r},\quad \beta = k_0^2 \varepsilon_r,\ g = j\omega\mu_0 J_z. \quad (5)$$

The weighted residual r^e for a single element over the domain Ω^e is defined as the difference between the left hand side terms and the right hand side term of (4),

$$r^e = \frac{\partial}{\partial x}\left(\alpha_x \frac{\partial u}{\partial x}\right) + \frac{\partial}{\partial y}\left(\alpha_y \frac{\partial u}{\partial y}\right) + \beta u - g. \quad (6)$$

As outlined above, our aim is to minimize this weighted residual, i.e., to have a lowest error as in the literature references.

By multiplying this residual, (6), with a weight function w, integrating over the domain Ω^e, and putting the integral equal to zero, we obtain

$$\iint_{\Omega^e} w\left[\frac{\partial}{\partial x}\left(\alpha_x \frac{\partial u}{\partial x}\right) + \frac{\partial}{\partial y}\left(\alpha_y \frac{\partial u}{\partial y}\right) + \beta u - g\right] dxdy = 0. \quad (7)$$

Using the Green's Theorem and replacing the weight function w and u by the shape function N_i and $\sum_{j=1}^{n} \boldsymbol{u}_j^e \boldsymbol{N}_j$ respectively, (7) becomes

$$\begin{aligned} &-\iint_{\Omega^e}\left[\alpha_x \frac{\partial N_i}{\partial x}\frac{\partial\left(\sum_{j=1}^{n} u_j^e N_j\right)}{\partial x} + \alpha_y \frac{\partial N_i}{\partial y}\frac{\partial\left(\sum_{j=1}^{n} u_j^e N_j\right)}{\partial y}\right] dxdy \\ &+\iint_{\Omega^e} \beta N_i \left(\sum_{j=1}^{n} u_j^e N_j\right) dxdy \\ &= \iint_{\Omega^e} N_i g dxdy - \oint_{\Gamma_e} N_i \left(\alpha_x \frac{\partial u}{\partial x} n_x + \alpha_y \frac{\partial u}{\partial y} n_y\right) dl, \\ &\qquad for\ i = 1,2,...,n \end{aligned} \quad (8)$$

which can written in a matrix form as

$$\begin{bmatrix} M_{11}^e & M_{12}^e & \cdots & M_{1n}^e \\ M_{21}^e & M_{22}^e & \cdots & M_{2n}^e \\ \vdots & \vdots & \ddots & \vdots \\ M_{n1}^e & M_{n2}^e & \cdots & M_{nn}^e \end{bmatrix} \begin{Bmatrix} u_1^e \\ u_2^e \\ \vdots \\ u_n^e \end{Bmatrix} + \begin{bmatrix} T_{11}^e & T_{12}^e & \cdots & T_{1n}^e \\ T_{21}^e & T_{22}^e & \cdots & T_{2n}^e \\ \vdots & \vdots & \ddots & \vdots \\ T_{n1}^e & T_{n2}^e & \cdots & T_{nn}^e \end{bmatrix} \begin{Bmatrix} u_1^e \\ u_2^e \\ \vdots \\ u_n^e \end{Bmatrix} = \begin{Bmatrix} f_1^e \\ f_2^e \\ \vdots \\ f_n^e \end{Bmatrix} + \begin{Bmatrix} p_1^e \\ p_2^e \\ \vdots \\ p_n^e \end{Bmatrix} \quad (9)$$

where

$$M_{ij}^e = -\iint_{\Omega^e}\left[\alpha_x \left(\frac{\partial N_i}{\partial x}\right)\left(\frac{\partial N_j}{\partial x}\right) + \alpha_y \left(\frac{\partial N_i}{\partial y}\right)\left(\frac{\partial N_j}{\partial y}\right)\right] dxdy, \quad (10)$$

$$T_{ij}^e = \iint_{\Omega^e} \beta N_i N_j dxdy, \quad (11)$$

$$f_i^e = \iint_{\Omega^e} N_i g dxdy, \quad (12)$$

$$p_i^e = -\oint_{\Gamma_e} N_i \left(\alpha_x \frac{\partial u}{\partial x} n_x + \alpha_y \frac{\partial u}{\partial y} n_y\right) dl. \quad (13)$$

and in a more compact form

$$\begin{bmatrix} K_{11}^e & K_{12}^e & \cdots & K_{1n}^e \\ K_{21}^n & K_{22}^e & \cdots & K_{2n}^e \\ \vdots & \vdots & \ddots & \vdots \\ K_{n1}^e & K_{n2}^e & \cdots & K_{nn}^e \end{bmatrix} \begin{Bmatrix} u_1^e \\ u_2^e \\ \vdots \\ u_n^e \end{Bmatrix} = \begin{Bmatrix} b_1^e \\ b_2^e \\ \vdots \\ b_n^e \end{Bmatrix} \quad (14)$$

with

$$K_{ij}^e = M_{ij}^e + T_{ij}^e,\ b_i^e = f_i^e + p_i^e. \quad (15)$$

C. Dirichlet Boundary conditions

The total electric field tangential to the PEC surface Γ_1 must vanish [1]. Thus, on the cylinder antenna boundary where radius a=0.6045 mm [8], we choose total z-directed field equal to zero,

$$E_z = 0 \quad over \quad \Gamma_1 . \tag{16}$$

This zero value is imposed for implementing the code in Matlab language and for each node lying on Γ_1.

D. Absorbing Boundary Conditions (ABC)

We truncate the geometry at ρ=60 mm, because the calculator is limited, and we must have the physical continuity of propagation at the same time, without any reflection or refraction at the fictitious boundary, that can perturb our simulation. For this, we use a kind of boundary conditions, noun as ABC which are the third kind or mixed boundary conditions, in the following form

$$\alpha \frac{\partial u}{\partial \rho} + \gamma u = q \quad over \quad \Gamma_2 . \tag{17}$$

The ABC used in this work are the first order as described in Refs. [9-13].

III. Results and Discussions

A. Mesh Generation

We use a double precision variable position p, that contains the x and y coordinates. This positions are generated by the Persson's mesh generator [14], which we ameliorate and adapt [15] to our geometry for the horizontal plane, shown in Fig. 3. We use two circular shapes, first one has a radius a=0.6045 mm and contains eight nodes at the Dirichlet boundary Fig. 4. Second circle has a radius ρ=60 mm and corresponds to the virtual boundary of the system where we impose the ABC. In this boundary we obtain 56 nodes, as shown in Fig. 3. We use for the mesh generation the adaptive Delaunay

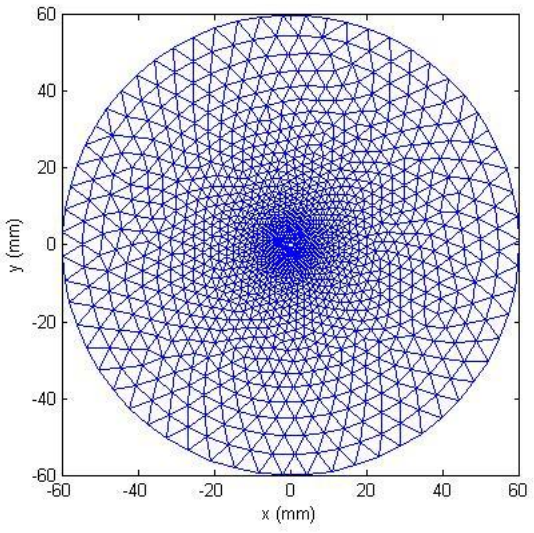

Figure 3. The horizontal plane mesh

triangulation [15] and we begin with an edge size equal to 0.5 mm. The mesh quality obtained is equal to 0.7980. The number of nodes generated is equal to 1330 and the

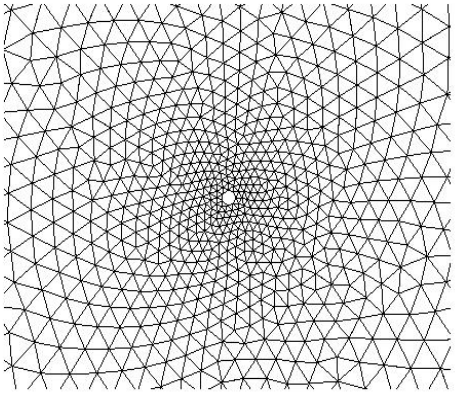

Figure 4. The horizontal plane mesh

elements number is 2592, done after 1541 iterations in 66.9301s.

For the vertical plane, we use two identical rectangular shapes with a gap equal to 0.125 mm, as shown in Fig. 5 and Fig. 6. This two rectangles are modeled inside a circular shape, which play the same role of ABC boundary, where ρ=60 mm. The rectangular shapes have a size equal to 30.225 mm × 1.209 mm. It is important to note that we have chosen a distance between the dipole and the ABC boundary equal to λ/4 [16]. We generate our mesh over this shape Fig. 6, and we obtain 2361 nodes, which give 3599 triangular elements. For the Dirichlet boundary we obtain 1088 nodes, and for the ABC we obtain 34 nodes. We begin the adaptive Delaunay triangulation with an edge size equal to 0.1 mm. The mesh quality obtained is equal to 0.0242. The mesh is obtained after 16340 iterations in 226.3033 s. Note that TAB. I. summarizes all

TABLE I.
MESH GENERATION DETAILS AND CPU TIME

CPU Time for Mesh Generation	Hor. plane		66.9301 s
	Ver. Plane		226.3033 s
Mesh Quality (finesse)	Hor. Plane		0.7980
	Ver. Plane		0.0242
Error Tolerance (ε)	0.01		
Iterations	Hor. Plane		1541
	Ver. Plane		16340
Elements Shape (simplexes)	Triangular		
Triangulation Method	Adaptive Geometrical Delaunay		
Initial Edge Size	Hor. Plane		0.5 mm
	Ver. Plane		0.1 mm
Shapes	Circle 1	Radius	60 mm
	Circle 2	Radius	0.6045 mm
	Rectangle 1	30.225x1.209 mm	
	Rectangle 2	30.225x1.209 mm	
Nodes Number (positions P)	Hor. Plane		1330
	Ver. Plane		2361
Simplexes Number (t)	Hor. Plane		2592
	Ver. Plane		3599
Dirichlet Boundary Nodes Number	Hor. Plane		8
	Ver. Plane		1088
ABC Boundary nodes Number	Hor. Plane		56
	Ver. Plane		34

information related to mesh generation of this work.

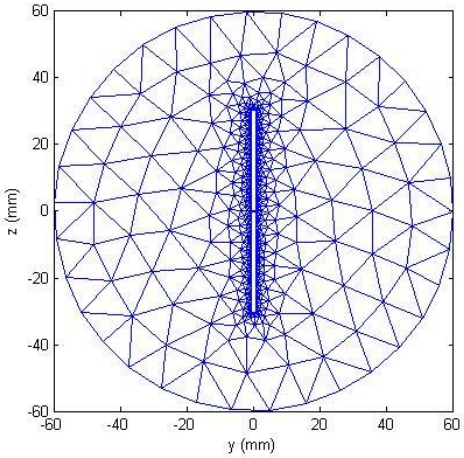

Figure 5. The vertical plane mesh

B. Finite Element Solution

Once we obtain coordinates, positions, and simplexes arrays we proceed to implement our finite element solution by choosing the different parameters and implement the procedure given in the section above. The code used was created by Polycarpou [1]. We ameliorate this code by choosing proper implementations for the boundary nodes selection and we adapt this code to simulate effects of electric density excitation [4].

We choose μ_r and ε_r equal to one, according that the antenna radiates in free space [17]. The amplitude E_0=1V/m, $k_0=2\pi/\lambda$, and since we are modeling 2400 MHz dipole antenna, λ=120.9 mm.

We simulate our antenna model for the horizontal plane and the vertical plane. We obtain results after 0.5907 s for the horizontal plane, and 13.1482 s for the vertical plane. The solution is obtained by the use of LAPACK library incorporated in Matlab. Finite element results are shown in Fig. 7 and Fig. 8.

In parallel to the finite element dipole antenna modeling, we simulate an electric field radiated by a dipole antenna, with the 4NEC2 software [8], which uses the method of moments (MoM) [18,19], and we compare our results with those obtained by the MoM simulation, as shown in Fig. 9.

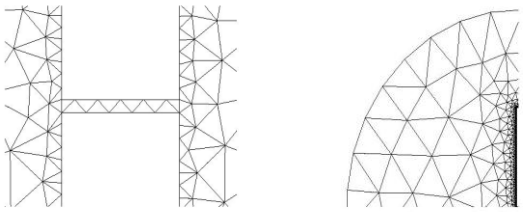

(a) (b)

Figure 6. The vertical plane mesh: (a) Gap distance between the rectangles and (b) Details about the dipole mesh

The maximum amplitude of the electric field is 70 V/m for the horizontal plane, Fig. 7. This is conforming to the MoM result, as shown in Fig. 10(b). For the vertical plane Fig. 8, we obtain the maximum amplitude for the electric field equal to 63.17V/m.

Fig. 9(a)-(b) show that the polar plot of our dipole antenna has an omnidirectional pattern. This antenna is not directive in the horizontal plane, and directional at any orthogonal plane. This kind of antennas has a space filter behavior. Because of the antenna symmetry around z-axe, the radiation is omnidirectional, and present a linearly polarization of the electric field.

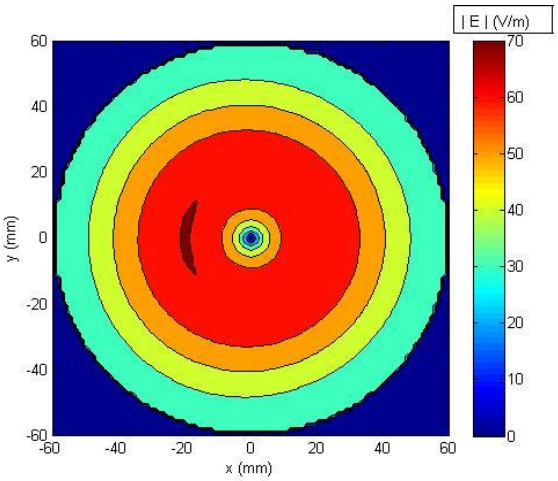

Figure 7. The horizontal plane contour plot of the total electric field based on a finite element solution

Fig. 8 shows the vertical plane contour plot of the total electric field based on finite element solution, and Fig. 9(c) shows the polar plot of the total electric field and it is in good agreement with the electric field obtained by the MoM method shown in Fig. 9(d).

The simulation based on the MoM method was successful with the use of the notepad card. In fact, the 4NEC2 software uses a card which contains all information

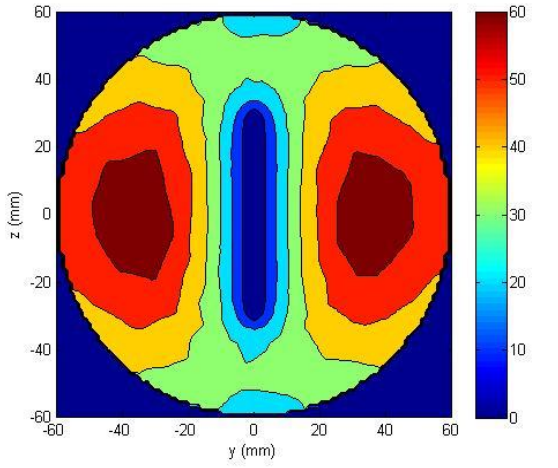

Figure 8. The vertical plane contour plot of the total electric field based on a finite element solution

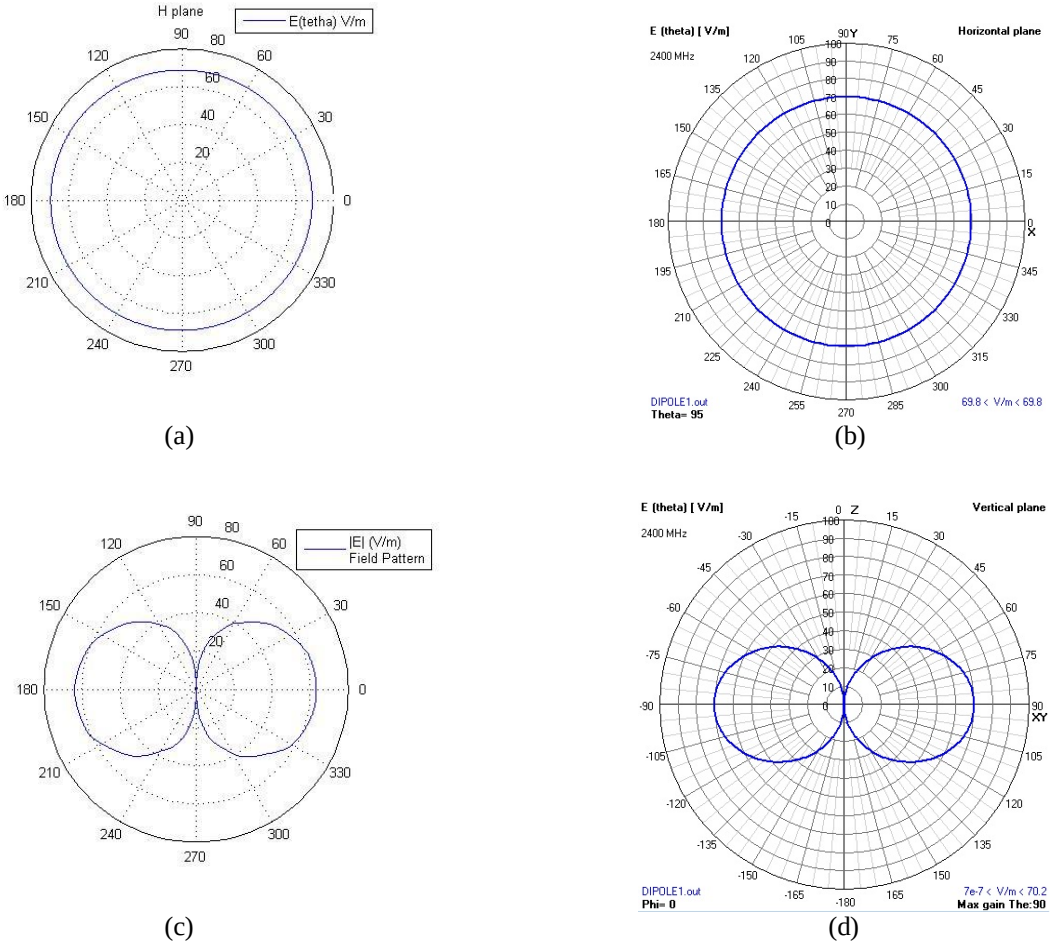

Figure 9. The polar plot of the total electric field for the horizontal plane: (a) finite elements solution, (b) moments method solution. The polar plot of the total electric field for the vertical plane: (c) finite elements solution, (d) moment's method solution

TABLE II.
CARD USED TO SIMULATE THE DIPOLE ANTENNA BASED ON THE MOM SOLUTION

```
CM Dipole in free space, converted with 4nec2 on june 13, 2015
CM      Dipole1
CM This is a dipole in free space.
CM The frequency is 2400MHz corresponding to lambda=120.9 mm.
CM Note that this antenna,
CM exactly a half wavelength long
CE
SY len=0.06045
GW      1       11      0       0       -len/2  0       0
len/2   0.6045e-3
GE      0
GN      -1
EK
EX      6       1       6       0       1       0       0
FR      0       0       0       0       2400    0
EN
```

related to geometry, frequency, material, ground, and excitation. For our simulation we use the card shown in TAB. II.

For the MoM model we used a half wavelength, and we choose radius equal to 0.6045 mm, geometry model is shown in Fig. 10(a). The current source has a real part equal to 1A, no imaginary part, and a magnitude equal to 1A, the phase is equal to zero.

According to our antenna problem, frequency is equal to 2400 MHz, which radiates in free space. The MoM simulation is generated over a tridimensional free space according to the x, y and z axes as shown in Fig. 10(c), where the total electric field pattern presents the omnidirectional characteristic of half wavelength dipole antennas. Fig. 10(d) shows the polar plot for both horizontal and vertical electric field, and the maximum corresponds to E=70 V/m.

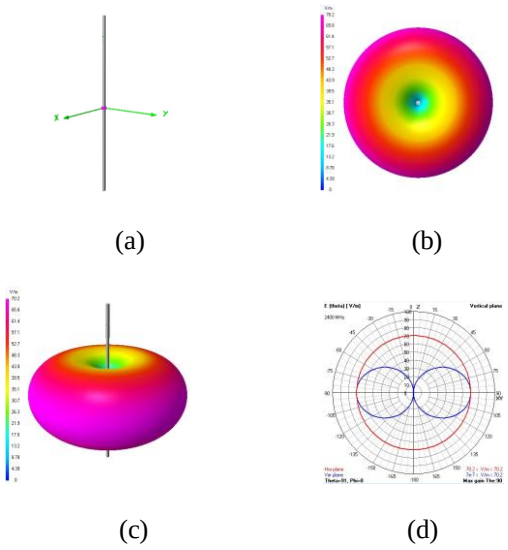

Figure 10. (a) 4NEC2 antenna geometry model. (b) Horizontal plane interpolation plot of the total electric field based on a MoM solution. (c) Tridimensional electric field pattern. (d) Polar plot of electric pattern in both horizontal and vertical plane.

IV. CONCLUSIONS

By using a fine description and implementing the Matlab code for the finite element at 2400 MHz dipole antenna modeling. We obtain results, which are comparable to those existing in literature and with those obtained with the MoM 4NEC2 software. This work can be used as the start for more complicated geometry antennas and more specifically electromagnetic antenna problems. The work made is a solution for the engineering need. We show that the minimization of the weighted residual tend to decrease the problem difficulty.

REFERENCES

[1] A. C. Polycarpou, "Introduction to the finite element method in electromagnetics," Synthesis Lectures on Computational Electromagnetics, vol. 1, no. 1, pp. 1-126, 2006.
[2] L. Bousshine, "The finite element method," ENSEM Hassan II University, Casablanca, Morocco, unpublished.
[3] J. P. A. Bastos and N. Sadowski, "Electromagnetic modeling by finite element methods," Marcel Dekker, Inc. 2003.
[4] E. El Kennassi and L. Bousshine, "The finite element method for electric field modeling near a cylinder," [3ème Edition du Workshop Modélisation Mathématique, Informatique et Analyse numérique, Errachidia, Morocco, 2015].
[5] J. Jin, "The finite element method in electromagnetics," John Wiley and Sons, Inc. Second Edition, 2002.
[6] C. A. Balanis, "Modern antenna handbook," John Wiley and Sons, Inc. 2008.
[7] M. N. O. Sadiku, "Numerical techniques in electromagnetics second edition," CRC Press LLC, 2011.
[8] 4NEC2, "American wire gauge table".
[9] A. F. Peterson, "Absorbing boundary conditions for the vector wave equation," Microwave and Optical Technology letters, vol. 1, no. 2, april 1988.
[10] A. Bayliss, M. Gunzburger and E. Turkel, "Boundary conditions for the numerical solution of elliptic equations in exterior regions," NASA Langley Research Center, Report no. 80-1, January 11, 1980.
[11] A. Bayliss and E. Turkel, "Radiation boundary conditions for wave-like equations," Communications on Pure and Applied Mathematics, John Wiley and Sons, Inc. vol. XXXIII, pp. 707-725, 1980.
[12] B. Engquist and A. Majda, "Absorbing boundary conditions for the numerical simulation of waves," Mathematics of Computation, vol. 31, no. 139, pp. 629-651, july 1977.
[13] J. P. Webb and V. N. Kanellopoulos, "absorbing boundary conditions for finite element solution of the vector wave equation," Microwave and Optical Technology letters, vol. 2, no. 10, October 1989.
[14] P. Persson and G. Strang, "A simple mesh generator in MATLAB," SIAM Review, vol. 46, no. 2, pp.329-345, 2004.
[15] E. El Kennassi and L. Bousshine, "Three-dimensional mesh generation using Delaunay triangulation," IOSR Journal of Mechanical and Civil Engineering, vol. 11, issue 6, ver. V, pp. 67-72, December 2014.
[16] Ansoft, "Antenna RF training guide," ANSYS Inc. 2010.
[17] ANSYS HFSS, "Materials characteristics table".
[18] G. J. Burke and A. J. Poggio, "Numerical electromagnetic code (NEC) method of moments," Lawrence Livermore Laboratory, Interaction notes Livermore, California, July 1977.
[19] G. J. Burke and A. J. Poggio, "Numerical electromagnetic code (NEC) method of moments," Lawrence Livermore Laboratory, Report UCID 18834, January 1981.